

Depths of melting and melt extraction beneath mid-ocean ridges as recorded in melt inclusions

N. Shimizu

Woods Hole Oceanographic Institution, Woods Hole, MA
02543, USA.

Recent studies have shown that chemical compositions of primitive melt inclusions in olivine and plagioclase phenocrysts in mid-ocean ridge basalts (MORB) carry important information of process of melting and melt extraction beneath mid-ocean ridges (e.g., Sobolev and Shimizu, 1993). It is generally observed that variations of trace element abundances and abundance ratios in melt inclusions on small sampling scales (e.g., single dredge, single pillow) are very large, and can be adequately explained by melting models involving efficient extraction of small-degree melt fractions. This paper reports chemical variations in two primitive melt inclusion suites (33.7°S, Mid-Atlantic Ridge and 36.5°N, Mid-Atlantic Ridge, FAMOUS area) with distinct trace element characteristics, representing melting and melt extraction occurred at different depths.

Major element compositions in melt inclusions and host minerals were determined with a JEOL 733 at MIT, and trace element abundances (Ti, V, Cr, Sr, Y, Zr, REE) were determined with a Cameca IMS 3f at WHOI. Only perfectly glassy primary inclusions were analyzed. Effects of post-entrapment growth of host minerals were found to be typically 5~15%.

Olivine ($_{89-91}$)- and plagioclase ($_{An_{81-88}}$)-hosted melt inclusions from four separate blocks of primitive basalt (Mg# ~72) recovered from a single dredge (AII 107.7, D20) at 33.7°S, MAR show the following ranges in trace element abundances and abundance ratios: 3100–6780 ppm Ti; 24.7–64.4 ppm Zr; 50.2–99.3 ppm Sr; 80–160 Ti/Zr (cf. average NMORB = 95; Hofmann, 1988); 0.32 - 0.79 [La/Sm]_n (cf. average N-MORB = 0.65). It is noticeable that plagioclase-hosted inclusions tend to have slightly higher incompatible element abundances than olivine-hosted ones and that olivine-hosted inclusions in a single pillow cover essentially the entire range. Negatively correlated large variations of Ti/Zr and [La/Sm]_n argue against low-pressure crystal fractionation, post-entrapment crystal growth and entrapment of evolved 'boundary layer' melt.

Olivine ($_{Fo_{89-91}}$)-hosted melt inclusions from a primitive basalt (ALV 519-4-1; Mg# = 68) at

36.5°N, MAR contain two distinct populations: (1) those with high incompatible element abundances, LREE enrichment ([La/Sm]_n up to 1.8), and chondritic Ti/Zr (~110), called E-melts; (2) those with low incompatible element abundances, LREE depletion ([La/Sm]_n ~0.3) and high Ti/Zr (up to 180), called D-melts. It appears that both

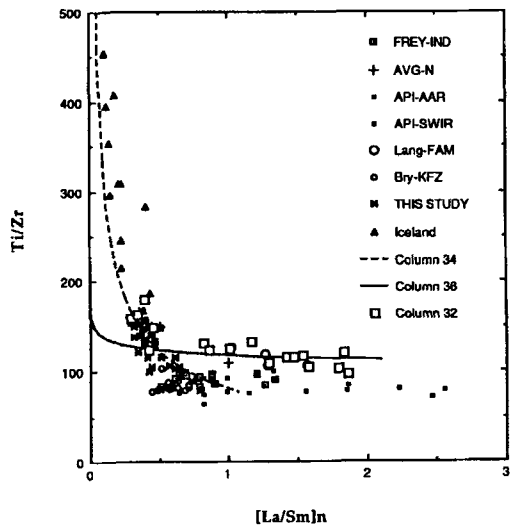


Fig. 1. Ti/Zr vs [La/Sm]_n of melt inclusions from a basalt (ALV 519-4-1) from FAMOUS (open squares, column 32), and from four blocks of basalt from a dredge (AII 107.7, D20) from MAR (barred x's, THIS STUDY) compared with selected MORB glass and whole-rock data from literature. FREY-IND: N. W. Indian Ocean (Frey *et al.*, 1980); API-AAR and API-SWIR (le Roex *et al.*, 1983); Lang-FAM (Langmuir *et al.*, 1977); Bry-KFZ (Bryan *et al.*, 1981); Iceland (melt inclusion data, Sobolev, unpublished). A dashed curve is a trajectory of instantaneous melts produced by critical (continuous) melting of depleted mantle (2 wt% retained melt) with spinel lherzolite residue. A flat-lying solid curve is a trajectory of instantaneous melts produced by critical (continuous) melting of the same depleted mantle (1 wt% retained melt) with garnet lherzolite residue.

types occur with almost equal frequency and that the E-melts tend to form larger (> 150 microns across) inclusions. Melt inclusions with intermediate characteristics also occur.

Salient features of the observed trace element characteristics are shown in Fig. 1. It is clear that the two populations of inclusions from the FAMOUS basalt define two distinct arrays, and the southern Atlantic suite plot together with the D-melts. Also note that ultra-depleted melt inclusions from Iceland (Sobolev, unpublished data) plot on an extension of the D-melt array.

These arrays can be compared well with trajectories of instantaneous melts produced in critical (continuous) melting of depleted mantle source ($[La/Sm]_n = 0.5$ and $Ti/Zr = 150$, estimated on the basis of $^{143}Nd/^{144}Nd$ and trace element abundance pattern of the source) at different depths. Partition coefficients of Ti and Zr between garnet and melt significantly reduces fractionation of these elements in successive melt fractions during critical melting, thereby producing a flat-lying trajectory in Fig. 1 for melts produced at depths where garnet is present as a residual phase. In contrast, melting at shallow levels produce a steep trajectory, and indeed ultra-depleted melts formed at advanced stages of melting in the uppermost mantle (e.g., Sobolev and Shimizu, 1993) plot on this trajectory.

It is suggested that trace element variations observed in melt inclusions can be interpreted as primary features of melting process, and that they can even retain record of initial stages of melting process occurred at great depths. The observations also suggest that these melt fractions were extracted from residues at depths and transported individually without complete equilibration with the wall-rock mantle until entrapment in high-Mg olivines at shallow level.

References

- Bryan, W. B., Thompson, G., Ludden, J. N. (1981) *J. Geophys. Res.*, **86**, 11815–36.
- Frey, F. A., Dickey, J. S., Thompson, G., Bryan, W. B., Davies, H. (1980) *Contrib. Min. Pet.*, **74**, 387–402.
- Hofmann, A. W. (1988) *Earth Planet. Sci. Lett.*, **90**, 297–314.
- Langmuir, C. H., Bender, J. F., Bence, A. E., Hanson, G. N., Taylor, S. R. (1977) *Earth Planet. Sci. Lett.*, **36**, 133–56.
- le Roex, A. P., Dick, H. J. B., Erlank, A. J., Reid, A. M., Frey, F. A., Hart, S. R. (1983) *J. Pet.*, **24**, 267–318.
- Sobolev, A. V., Shimizu, N. (1993) *Nature*, **363**, 151–4.